The Intermediate Temperature Deformation of Ni-Based Superalloys: Importance of Reordering

L. Kovarik, R.R. Unocic, J. Li, and M.J. Mills

A number of planar deformation mechanisms, such as microtwinning, a[112] dislocation ribbon, and superlattice intrinsic and superlattice extrinsic stacking fault formation, can operate during the intermediate temperature deformation of nickle-based superalloys. The fundamental, rate-limiting processes controlling these deformation mechanisms are not fully understood. It has been recently postulated that reordering of atoms in the wake of the gliding partial dislocations as they shear the γ′ precipitates within the γ/γ′ microstructure is the limiting process. Experimental evidence that substantiates the validity of the reordering model for the microtwinning mechanism is provided. A conceptual approach to study reordering at the atomic scale using ab-initio calculation methods is also presented. The results of this approach provide a clear conceptualization of the energetics and kinetics of the reordering process, which may be generically important for the aforementioned planar deformation modes.

INTRODUCTION

Nickel-based superalloys are a crucial class of metallic materials enabling present turbine engine designs for both aeronautics and energy generation. These alloys are essential due to their extraordinary combination of creep and fatigue strength. These remarkable properties are attributable largely to the presence of microscale and nanoscale populations of coherent γ′ ($L1_2$ structure) strengthening phases in a ductile face-centered cubic (fcc) matrix. Alloys designed for structural applications, such as disks and blades in aeroengines, must sustain large centrifugal stresses at high temperatures.

How would you…

…describe the overall significance of this paper?

Microtwinning is an important, but poorly understood, deformation mode for nickel-based superalloys deformed at intermediate temperatures. We have studied microtwinning down to the atomic level, and it has been unambiguously confirmed that its operation relies on thermally activated reordering within the γ′ precipitates in the wake of the twinning partials. The concept of reordering is relevant for other planar deformation mechanisms operating at intermediate temperatures in superalloys.

…describe this work to a materials science and engineering professional with no experience in your technical specialty?

Nickel-based superalloys are used predominantly in gas turbine engines due to their outstanding high strength and fatigue properties. Efforts to model service life and to improve the properties of these alloys require a fundamental understanding of deformation processes under creep and fatigue conditions. The reordering process described appears to be key to understanding the temperature-dependence of the strength of superalloys in this temperature range.

…describe this work to a layperson?

Improving the efficiency of turbine engines for both aerospace propulsion and land-based power generation requires materials that can withstand the incredible stresses and temperatures generated during fuel combustion. Superalloys are the only materials that provide the required strength and performance. This study provides fundamental insight that may allow the design of superalloys with even better properties.

Deformation mechanisms of nickel-based superalloys have been extensively studied in the past. At lower temperatures and higher stresses, shearing of the γ′ precipitates occurs via the coupled movement of paired a/2<110> dislocations[1,2] while at much higher temperatures (around 800°C), climb bypass of the γ′ precipitate by individual, unpaired a/2<110> dislocations is predominant.[3]

In the temperature range between anti-phase boundary (APB) shearing and climb bypass processes, several other mechanisms have been identified. One of the most remarkable is microtwinning,[4–7] which imparts very thin twins (microtwins) on the order of 2−50 atomic planes on the deformed microstructure. The other possible shearing mechanisms involve formation of either superlattice intrinsic stacking faults (SISF) or superlattice extrinsic stacking faults (SESF).[7–9] These faults can have either an isolated character (only in γ′) or can be extended and traverse both matrix and precipitates. Deformation mechanisms that involve temporary formation of both fault types are often referred to as the "stacking fault ribbon" mechanisms. This was initially documented by B.H. Kear[2,10] and is due to the operation of a<112> perfect matrix dislocations that shear the γ′ particles by forming SISF and SESF pairs within the γ′ precipitates.

This paper focuses on the rate-limiting process for the planar deformation mechanisms, with special attention on microtwinning. Experimental evidence is presented that demonstrates reordering within the γ′ precipitates to be the rate-limiting process in microtwinning. This recently discovered process enables microtwinning, and possibly sev-

eral other γ′ shearing mechanisms, to operate at intermediate temperatures and may define the practical, upper-bound temperature for the utilization of these alloys.

MICROTWINNING MECHANISM

The polycrystalline alloy Rene 104 undergoes microtwinning at stresses of approximately 690−724 MPa and a temperature of 677°C. At this temperature and stress, microtwinning is found to be the dominant deformation mechanism in a substantial number of grains. The deformation structure of a typical grain that undergoes microtwinning is shown in Figure 1a. The planar faults in this micrograph are microtwins, which are present in two different orientations (lying on two different {111} type planes). Some are imaged in a nearly edge-on orientation while the microtwin in the center of the image is inclined, revealing a fringing pattern. High-resolution imaging confirms that the planar faults are indeed microtwins. An example of a microtwin stretching across a γ′-precipitate is shown in Figure 1b. Microtwins shear both the γ and γ′ phases, and at larger strains of the order of 1%, the microtwins usually extend across entire grains. These microtwins are much thinner than the annealing twins that are also common in these alloys and are definitively associated with deformation at this intermediate temperature. It is found that a majority of the twins in the γ′ phase have an even number of layers and that their thickness can vary, with a majority of them being in the range of 4−50 layers thick.

The nature of the twinning partial dislocations is key to understanding why microtwinning may be a thermally activated process that occurs only at elevated temperature. High-resolution imaging has been able to provide definitive proof regarding the detailed nature of the twinning partials, augmenting earlier diffraction contrast transmission electron microscope (TEM) analysis by several groups.[5,7] An example of a microtwin in the γ′-phase that contains several twinning dislocations is shown in Figure 2. These are high-angle annular dark field (HAADF) images obtained using an FEI Titan 80−300 scanning TEM with c_s-correction on the electron probe, operating at 300 kV. The HAADF imaging reveals the core of the twinning partial dislocation. At the location of the twinning partials, the microtwin changes thickness. In the observations provided in Figure 2a, the microtwin changes from two to four layers and in Figure 2b it changes from four to six layers. In both cases, two twinning partial dislocations are observed in close proximity to one another. While this fact may not be immediately apparent from the as-acquired images, it becomes more evident in Figure 2c and d where the same images have been color-coded based on the central/inversion symmetry. Blue represents the symmetry of the perfect crystal, while "warmer" colors represent deviation from the perfect crystal symmetry. The color representation enables us to visually establish that the separation between the Shockley partials is very small—less than 1.5 nm in one case and virtually "compact" in the other case.

Drawing the Burgers circuit and encompassing the twinned region reveals that the edge component of the two partials is b_e=1/6[112]. Given the value of the edge component, it can be concluded that both twinning partial dislocations must be 1/6[112] dislocations that are viewed in the 30º orientation. In this orientation, the 1/6[112] Shockley partials can be distinguished from 1/3[112] partial dislocations, which are the other possible partial dislocations that could shear the precipitates.[5] The high-resolution images unambiguously confirm that the operative dislocations are two 1/6[112] Shockley partials.

THERMALLY ACTIVATED SHEARING

These high-resolution imaging results support the model by M. Kolbe,[11] and more recently by S. Karthikyen et al.,[12] who suggest that reordering is the rate-limiting process for the microtwinning deformation mechanism. The reordering process transforms the high-energy fault created by the gliding Shockley partial dislocations into a lower-energy counterpart via a local diffusion. The former has a higher energy since numerous unfavorable nearest neighbors are created when the γ′ is sheared by a Shockley partial dislocation, as is discussed further in the next section.

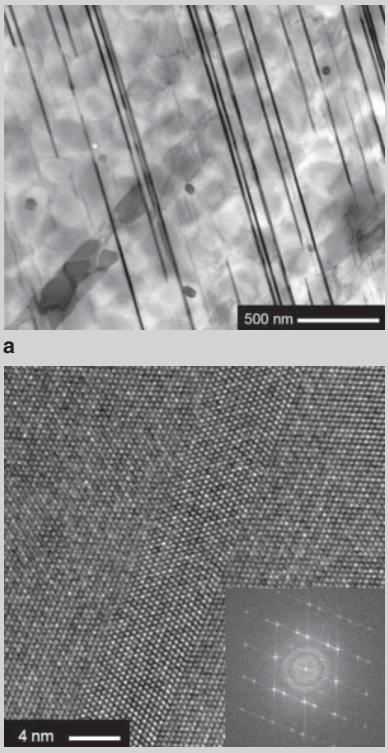

Figure 1. (a) A general view of the deformed microstructure revealing microtwins in edge-on and inclined orientation. (b) Microtwin in the γ′-phase that has a thickness of 14 layers. The insert is a Fourier transform confirming the presence of superlattice reflections of the γ′.

The premise of the reordering model is the following. Under the action of the applied shear stress, dislocations bow around larger (secondary) γ′ particles as the high-energy, two-layer complex stacking fault (CSF) prevents athermal cutting. A narrow entry into the γ′ is nevertheless established, the extent of which depends on the balance between the driving force of the dislocation segment and the drag force from the fault creation. Immediately in the wake of the two 1/6[112] dislocations, the fault energy can be lowered by reordering. This leads to a reduction of the drag force on the gliding dislocation, which in turn enables the dislocation pair's further advancement. A schematic of the dislocation cutting process is shown in Figure 3. The larger γ′ particles have been shaded depending on the energy of the fault: the darker the color, the higher the fault energy. The smaller γ′ particles are sheared athermally.

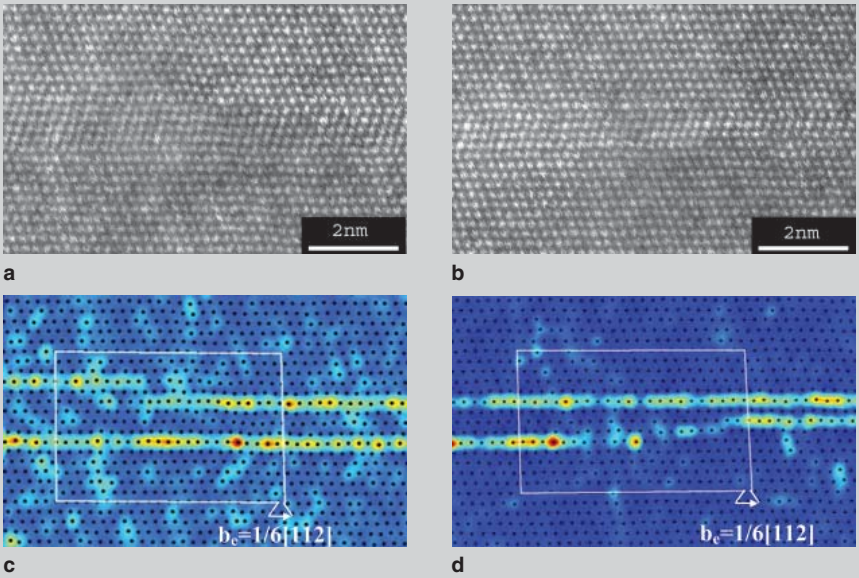

Figure 2. (a) An HAADF image depicting the presence of two 30° 1/6 [112] dislocations at the microtwin interface, changing the thickness from four to six layers. (b) An HAADF image depicting presence of two 1/6 [112] dislocations at the microtwin interface, changing thickness from two to four layers. (c,d) Corresponding RGB color-coded images based on central symmetry parameter highlighting the interface of the microtwin.

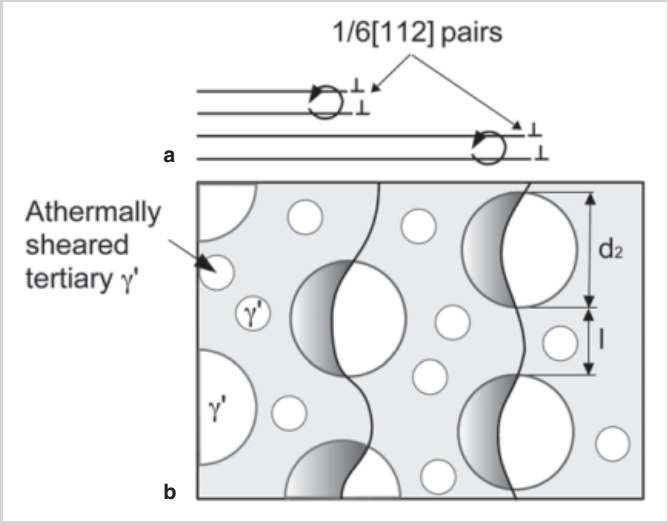

Figure 3. A schematic of the microtwinning mechanism and the geometry of the model. (a) Edge-on view (b) plan view of the leading partial dislocations in microtwin.

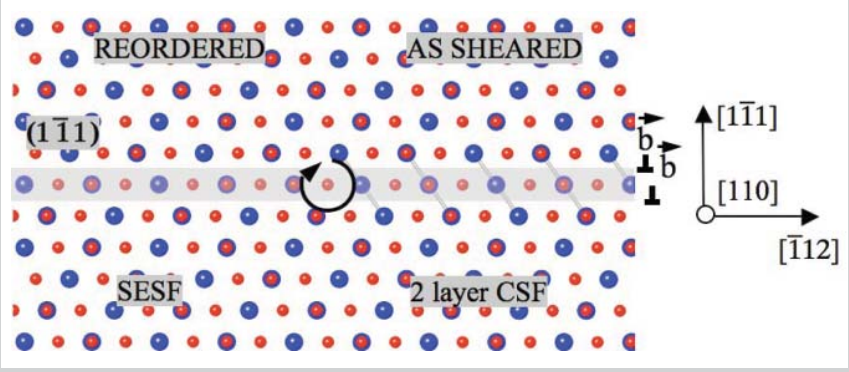

Figure 4. A two-layer fault created by passage of two 1/6 [112] partial dislocations from left-to-right on consecutive {111} glide planes, as viewed along the [110] direction. The unfavorable nearest-neighbor bonds created in the wake of the partial dislocations are identified in light grey.

ATOMIC ASPECTS OF REORDERING

Reordering of the faulted/twinned microstructure into a lower-energy configuration can proceed in a crystal that has been sheared by an even number of 1/6[112] dislocations.[7] The simplest configuration that can reorder from a high energy to a lower energy is thus a two-layer complex stacking fault. A schematic of this situation is shown in Figure 4 for the idealized case of ordered Ni_3Al (Cu_3Au structure). In this illustration, the high energy, two-layer CSF fault is on the right-hand side, while a lower energy SESF is shown on the left-hand side. The two faults differ since on the right-hand side there are unfavorable (high energy) nearest neighbor Al-Al bonds, while these bonds have been eliminated on the left-hand side by the reordering process (represented by the circular arrow). A similar reordering process is also possible following the passage of subsequent pairs of Shockley partials on consecutive planes.

Focusing on the two-layer fault, the reordering process requires reshuffling of atoms only in the central plane of the fault. A schematic depiction of the central plane is shown in Figure 5a. The essential feature of this plane is a row of anti-site point defects (Al^{Ni} and Ni^{Al}). The anti-site columns are in the closed-packed [110] direction and are perpendicular to the 1/6[112] Burgers vector. Reordering of the two-layer fault requires a simple exchange between aluminum and nickel atoms in the anti-site column of the plane as shown in Figure 5b. It should be noted that changing of aluminum and nickel in any other closed-packed [110] direction would not accomplish reordering into an SESF/true-twin configuration.

The reordering of aluminum and nickel atoms in a microtwin is a vacancy-mediated diffusion process. One can easily envision several ways in which the vacancy movement can accomplish the swap between the nickel and aluminum sites. In perhaps the simplest and most highly correlated case, the vacancy would move in the [110] direction as shown Figure 5c. As the vacancy moves along the [110] direction, the nickel and aluminum atoms

in the column will be placed into the neighboring sites and thus assume positions which are consistent with a low-energy SESF configuration. One can easily envision many more viable but less correlated vacancy paths that will accomplish the exchange of the nickel and aluminum sites. One such path is shown in Figure 5d. In this less correlated case, the vacancy will enter the mixed column via a nickel site, will accomplish one exchange between nickel and aluminum sites, and will exit from the mixed column. The descriptions provided here for reordering are different from the description provided previously by Kolbe.[11]

AB-INITIO STUDIES

Qualitative and quantitative evaluation of the reordering process requires understanding of the vacancy formation ΔG^f and vacancy migration ΔG^m energies associated with movement along the viable reordering paths. The energetic aspect of the vacancy exchanges allowing for reordering of nickel and aluminum sites can be studied with ab-initio calculations. For the purpose of ab-initio calculations, a super-cell of the faulted crystal of Ni_3Al was set up. The calculations were performed with the Vienna ab-initio Simulation Package (VASP).[13,14] The details of the calculations are provided elsewhere.[15]

There exist a variety of pathways that accomplish an exchange of the nickel and aluminum antisites. The reordering pathways considered presently assume that the starting point is such that the vacancy is on a nickel site adjacent to the anti-site column. The other possible scenarios with the vacancy on an aluminum site are not considered here. This assumption stems from the fact that a significantly higher concentration of vacancies exists on nickel sites in the model system, Ni_3Al.[16]

Given that the vacancy is on a nickel site, all viable pathways can be considered as a minimum three-step vacancy jump sequence. The first step always involves an exchange of the vacancy with an atom in the anti-site [110] column. The second step involves exchange of the vacancy and the second atom from the anti-site [110] column. This step places the second atom on its proper site. In the third step, the swap

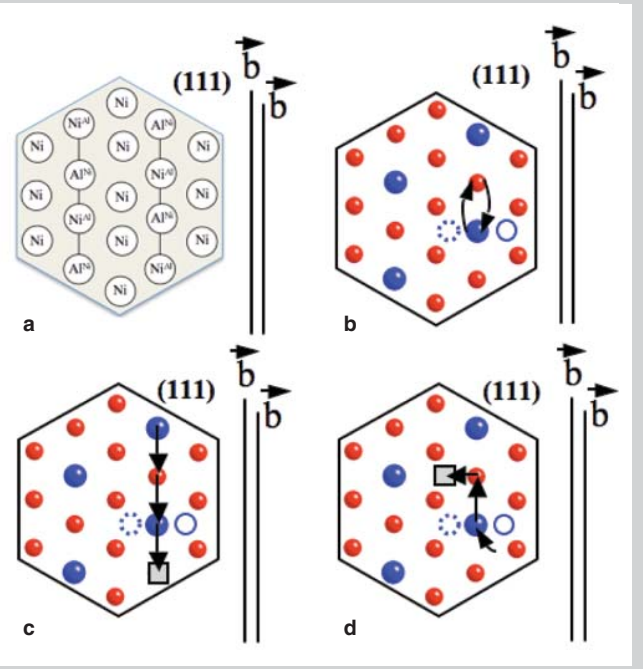

Figure 5. (a) Atom arrangement in the central plane of the two-layer complex fault. (b) Exchange of Al and Ni atoms that locally transforms the "as-sheared" into a "reordered" configuration. (c) Linear movement of vacancy in the [110] column of anti-sites that accomplish the transformation. (d) An example of a less correlated case allowing a single exchange between a pair of Al and Ni atoms. (The atom color-coding is nickel-red, aluminum-blue; empty circles are atoms from the plane above/below).

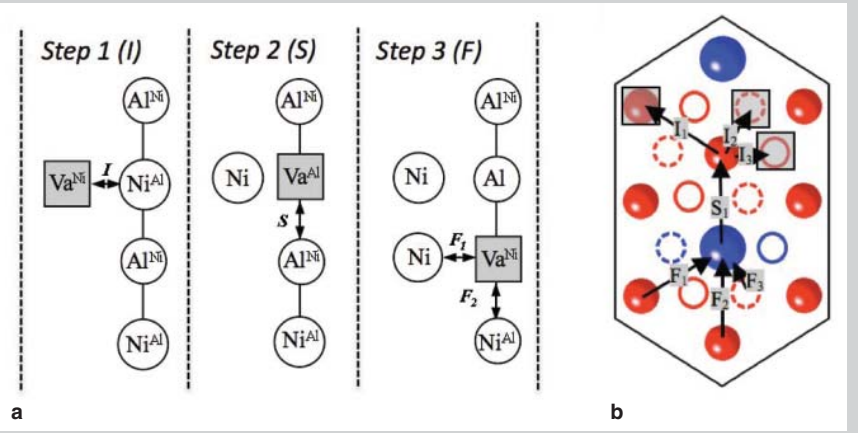

Figure 6. (a). A schematic of the reordering sequence initiated with an exchange between Va^{Ni} and Ni^{Al}. (b) The actual representation of the atom configuration and the possible reordering pathways. The atom color-coding is nickel-red, aluminum-blue.

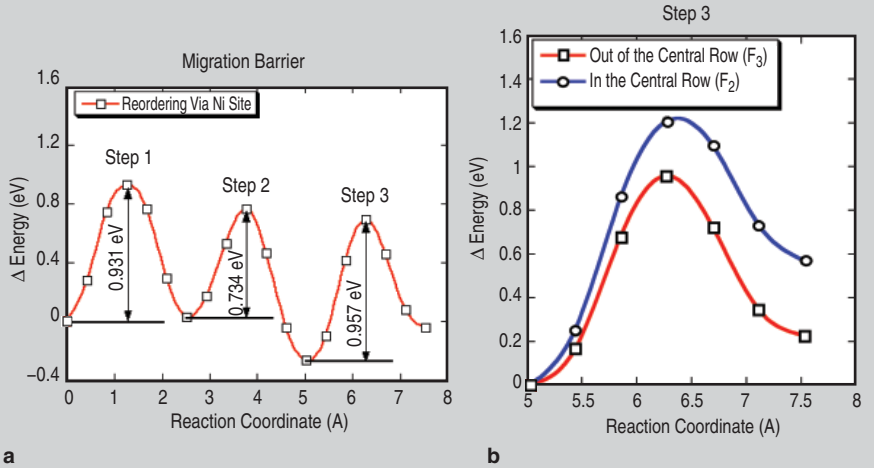

Figure 7. (a) The energy landscape associated with vacancy steps that accomplish a reordering of a single Al-Ni pair. The process initiates with an exchange between Va-Ni. (b) A comparison of the migration energy for step F_2 and F_3.

between the two anti-sites is accomplished.

An example of a jump sequence which initiates with the Va^{Ni}-Ni^{Al} exchange is shown in Figure 6a. Step 2 is an exchange between Va^{Al}-Al^{Ni} (places aluminum on the proper sub-lattice) and step 3 is Va^{Ni}-Ni^{*}, which puts nickel on the proper sub-lattice and thus accomplishes reordering of one Al-Ni pair. In the actual crystal, several nickel sites can be involved in the first and third exchanges. This can be well seen in the actual representation of the atomic arrangement in the central plane of the complex fault, as shown in Figure 6b. Please note that the atoms represented by empty circles (dashed and full) in this schematic are from the plane above and below, respectively.

The energy landscape corresponding to a sequence of jumps $I_1S_1F_3$ is shown in Figure 7a. Step I_1 has a migration barrier of 0.93 eV. Similar values of the migration energy are obtained for the initial exchange I_2 while the migration barrier associated with exchange I_3 is substantially larger, approximately 1.2 eV. The subsequent exchange S_1 is highly energetically favorable; the system lowers its energy by 0.297 eV. The energetic favorability of S_1 can be ascribed to the fact that one Al-Al nearest neighbor bond is eliminated in the system. The migration barrier (ΔG^m) associated with the jump is relatively low, having a value of 0.734 eV. The final exchange F_3 represents jumps with the nickel atom from the interface. The exchange increases the energy of the system by approximately 0.2 eV. The migration barrier associated with the exchange is 0.95 eV. The energy balance of the exchange F_1 is comparable to F_3, while the exchange F_2, which would allow for the linearly correlated diffusion in the anti-site columns (Figure 6b), has a migration barrier of approximately 1.2 eV, and energy balance of approximately 0.56 eV. Given these high values, it can be concluded that the linear motion of vacancy will not be the relevant mode of reordering.

KINETICS OF REORDERING

The calculation of migration energies for the viable reordering pathways serves two purposes. First, it enables the prediction of the most likely pathway the vacancy will take in reordering of Al-Ni atoms. Second, it provides a basis for the prediction of reordering kinetics.

The preliminary calculations suggest that the reordering processes will be analogous to the scenario depicted in Figure 5d.[15] This means that the vacancy will move in an uncorrelated manner, crisscrossing with multiple entries and exits from the central row of antisites. The entries will be favored through the Ni^{Al} anti-sites.[15]

The reordering kinetics can be estimated from the knowledge of activation energy ΔQ of the involved diffusion steps. The activation energy consists of vacancy formation and migration energy, $\Delta Q = \Delta G^{form} + \Delta G^{mig}$. Both values are different from the values in the bulk due to structural/chemical modification.

The vacancy formation energy ΔG^{form} at the nickel sites that are the starting point for the reordering were tested with ab-initio calculations. It was found that the formation energy is lower by approximately 0.1 eV with respect to the formation energy in the bulk. This fact will increase the concentration of vacancies and thus promote the reordering kinetics. On the other hand, the migration energy ΔG^{mig} will have an opposite effect on the kinetics. The ΔG^{mig} of the first step in the reordering sequence, which is the step that controls the kinetics of the sequence, is found to be approximately 0.1 eV higher than the migration barrier for a Va-Ni exchange in the bulk. Thus, the rate at which the vacancies will jump into the Ni^{Al} site and initiate the reordering will be lower than the jumps to the nickel site in the bulk.

By combining the values of ΔG^{form} and ΔG^{mig}, it is found that the activation energy for the first jump in the reordering sequence is similar to the activation energy for diffusion of nickel on its sublattice in the bulk. This is a very important result since it indicates that the reordering kinetics can be approximated using nickel self-diffusion in Ni_3Al. This conclusion represents a first approximation. It should be noted that this approximation does not account for the diffusion correlation effects, the alloy multi-component composition and, most importantly, the fact that the reordering could be taking place in the close vicinity of the dislocation core.

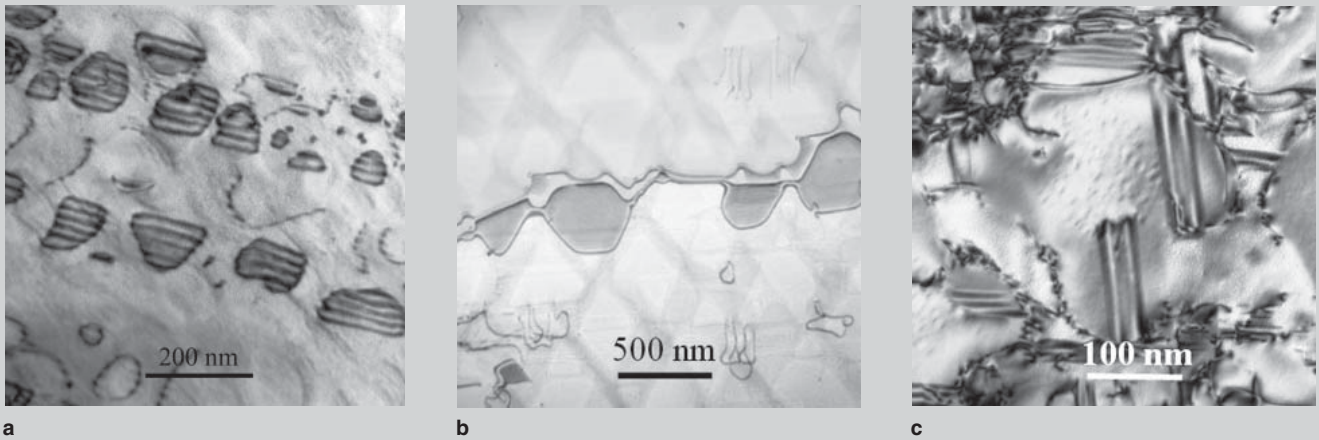

Figure 8. (a) Isolated faulting as observed by G.B. Viswanathan et al.[7] (b) Stacking fault ribbon as observed by C.M.F. Rae and R.C. Reed.[19] (c) SISF formation.

OTHER PLANAR DEFORMATION MECHANISMS

A variety of other planar deformation mechanisms have been reported to operate at intermediate/high temperatures in the γ/γ′ microstructure of nickel-based superalloys. The insights discussed above regarding reordering may also be key to understanding these mechanisms. They appear to progress in a viscous manner and be thermally activated.[7,17,18]

For example, one such deformation mechanism has been denoted as "isolated SESF formation;" a mechanism which leaves extrinsic faults in γ′. The individual SESFs can be grouped according to the location on (111) plane of the "γ/γ′-grain." Each group (family) belongs to one (111) plane and extends through a substantial part of the γ/γ′ microstructure.[7] An example of such a configuration is shown in Figure 8a. This configuration implies that the γ matrix has been sheared by a perfect lattice translation while the γ′ was sheared by a pair of 1/6[112] dislocations on consecutive planes. The shearing of γ′ is thus fully analogous to microtwinning.

Similarly, the formation of "dislocation ribbons" is known to be a key deformation mechanism in primary creep of single-crystal alloys in [100] near orientation. The importance of this mechanism was recognized in the early work by B.H. Kear at al.[17] and subsequently confirmed by others.[19] However, the rate-limiting process associated with this mechanism has yet to be clearly identified. An example of a dislocation ribbon is shown in Figure 8b. The Burgers vector of the dislocation ribbon is a[112], which is a perfect translation in the $L1_2$ ordered crystal structure. The propagation of the dislocation does not leave planar defects in the γ/γ′ structure but in its characteristic dissociated configuration consisting of superlattice intrinsic/extrinsic stacking fault (SISF/SESF) ribbon. The individual partial dislocation and fault components of this configuration can be expressed as: $1/3[\bar{1}12]$ & |SISF| & $1/6[\bar{1}12]$ & |APB| & $1/6[\bar{1}12]$ & |SESF| & $1/3[\bar{1}12]$.[19] The fine structure of the dislocation ribbon was previously studied by Kear.[10] The reported configuration is rather complex, composed of a series of partial dislocations gliding on two adjacent planes. The fact that this mechanism involves a complex arrangement of the Shockley partial dislocations and formation of SISF/SESF suggests that it is controlled by reordering in the wake of the moving partial dislocations. A schematic of the various steps involved in such a reordering-controlled deformation process for the complex dislocation ribbons is shown in Figure 9. A more complete discussion of this process is provided elsewhere.[15]

First-principles calculations have shown for the first time that the kinetics of reordering could be similar to that for nickel self-diffusion, at least for the simplified binary ordered γ′ structure considered presently.

Some single-crystal and polycrystalline nickel-based alloys with wider γ channels can initially deform by 1/2<110> dislocations in the γ matrix. While at small strains the deformation is fully accommodated by the activity in γ channels, at larger strains the deformation requires shearing of γ′ phase particles. The shearing of γ′ is often accomplished by 1/3[112] partial dislocations that leave SISF.[8,18] An example of SISFs in the γ′ is shown in Figure 8c. It is normally understood that the SISF form in the wake of 1/3[112] without a need for reordering. This would indeed be the case if the dislocation had a compact character or was dissociated on a single (111) plane. If the dislocation is split in the same manner as the leading segment in Figure 9, or in other words is in the Giamei lock configuration,[20] then reordering will be required for continuouss glide. Previous experimental and modeling work indicates that the Giamei lock core configuration can indeed be favored.[22,23]

CONCLUSIONS

Previous, detailed TEM studies of nickel-based superalloys have revealed that a rich variety of deformation processes can occur depending on deformation condition and microstructure. In this brief review, the occurrence of microtwinning as an important creep deformation mode at intermediate temperatures (~660−700°C) has been shown, and the hypothesis that the rate controlling process is due to reordering within the strengthening γ′ precipitates has been discussed. First-principles calculations have shown for the first time that the kinetics of reordering could be similar to that for nickel self-diffusion, at least for the simplified binary ordered γ′ structure considered presently. Furthermore, it is postulated that reordering could be at the heart of several other thermally activated mechanisms such as the isolated faulting and stacking fault ribbon configurations also observed at intermediate temperatures. A more complete understanding of the reordering process, and the effect of temperature and alloy chemistry, may therefore provide a possible unification of these apparently diverse mechanisms.

It is worthwhile to consider these mechanisms in the broader context of the other mechanisms that appear to dominate at different temperatures. At lower temperatures and high stress, shearing of the γ′ precipitates occurs by the coupled movement of pairs of 1/2<110> matrix dislocations, as illustrated in Figure 10a. An APB is created in the γ′ by the leading 1/2<110> dislocation. The APB is "repaired" by the trailing 1/2<110> dislocation. This mechanism does not depend on diffusion, although it may require local cross-slip in order to configure the dislocation pairs on the same slip plane. Therefore, this mechanism should not be as strongly temperature dependent as compared with the reordering-mediated shearing mechanisms, as illustrated in Figure 10b for SESF formation. At higher temperatures, above those where microtwinning and fault forma-

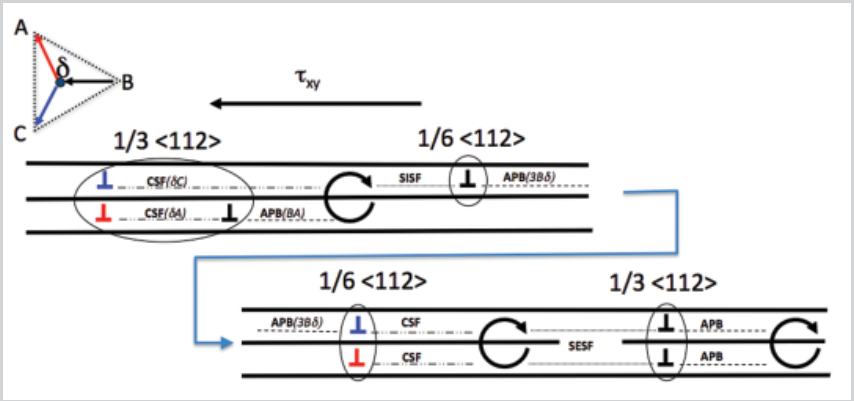

Figure 9. The schematic of the a[112] dislocation ribbon. The leading dislocation is a zonal a/3[112], which is separated by SISF from the next a/6[112]. The subsequent a/6[112] is separated by SESF from the next a/3[112].

tion are observed, deformation again appears to be controlled by operation of 1/2<110> matrix dislocations. However, rather than shearing the γ′ precipitates, the matrix dislocations can surmount the precipitates by local climb, as illustrated in Figure 10c. Climb over length scales similar to the γ′ particle size requires long-range diffusion. On this basis, it is sensible that the reorder-mediated processes discussed in this paper occur at a temperature intermediate between the APB-shearing and climb bypass regimes. Indeed, it could be argued that more complete understanding and control of the reordering process, and the associated deformation mechanisms, may provide critical insights in order to push the limits of disk alloys to higher operating temperatures than are presently achievable.

A complete, physics-based model of deformation in these complex alloys clearly will require consideration of these individual mechanisms, as well as the transitions between mechanisms as a function of temperature and microstructure. While there exists an enormous, empirically based understanding of alloy composition, microstructure, and properties in the disk superalloys, a fundamental understanding of the operative mechanisms over a broad range of deformation and microstructure conditions will require continued coordinated experimentation coupled with modeling at a variety of length scales.

ACKNOWLEDGEMENTS

The authors would like to acknowledge support from the U.S. Air Force Office of Scientific Research under the MEANS-2 program Grant No. FA9550-D5-1-0135.

References

1. H. Gleiter and E. Hornbogen, *Physica Status Solidi,* 12 (1965), p. 251.
2. B.H. Kear, J.M. Oblak, and A. Giamei, *Metallurgical Transactions,* 1 (1970), p. 2477.
3. T.M. Pollock and A.S. Argon, *Acta Metallurgica et Materialia,* 40 (1992), p. 1.
4. K. Kakehi, *Scripta Materialia,* 41 (1999), p. 461.
5. D.M. Knowles and Q.Z. Chen, *Materials Science and Engineering,* A340 (2003), p. 88.
6. G.B. Viswanathan et al., *Philosophical Magazine,* 86 (2006), p. 4823.
7. G.B. Viswanathan et al., *Acta Materialia,* 53 (2005), p. 3041.
8. Q.Z. Chen and D.M. Knowles, *Materials Science and Engineering,* 356 (2003), p. 352.
9. B. Decamps et al., *Philosophical Magazine,* 84 (2004), p. 91.
10. B.H. Kear and J.M. Oblak, *Journal de Physique Colloques,* 35 (1974), p. C7-35.
11. M. Kolbe, *Material Science and Engineering A,* 319-321 (2001), p. 383.
12. S. Karthikeyan et al., *Scripta Materialia,* 54 (2006), p. 1157.
13. G. Kresse and J. Furthmüller, *Comput. Mat. Sci.,* 6 (1996), p. 15.
14. G. Kresse and D. Joubert, *Phys. Rev. B,* 59 (1999), p. 1758.
15. L. Kovarik et al., *Progress in Materials Science* (submitted for publication).
16. C. Jiang, D.J. Sordelet, and B. Gleeson, *Acta Materialia,* 54 (2006), p. 1147.
17. B.H. Kear, G.R. Leverant, and J.M. Oblak, *Transaction of ASM,* 62 (1969), p. 639.
18. R. Unocic et al., *Superalloys 2008,* ed. R.C. Reed et al. (Warrendale, PA: TMS, 2008), p. 377.
19. C.M.F. Rae and R.C. Reed, *Acta Materialia,* 55 (2007), p. 1067.
20. A. Giamei et al., *Proc. 29th Annual Meeting EMSA* (Baton Rouge: Claitor's Publ., 1971), p. 112.
21. T. Link, *Scripta Metallurgica et Materialia,* 31 (1994), p. 671.
22. Y.Q. Sun, M.A. Crimp, and P.M. Hazzleidine, *Philosophical Magazine A,* 64 (1991), p. 223.
23. M. Yamaguchi et al., *Philosophical Magazine A,* 45 (1982), p. 867.

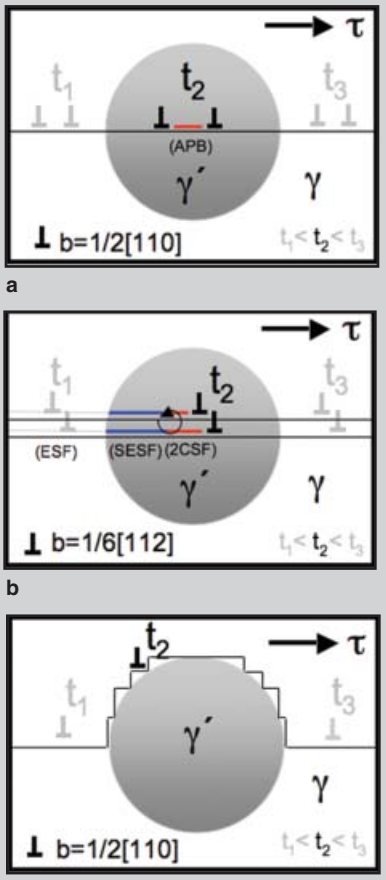

Figure 10. Deformation mechanisms of nickel-based superalloys in context of broader temperature range. (a) Dislocation APB shearing, (b) planar deformation (such as microtwinning), (c) dislocation climb by-pass.

L. Kovarik, R.R. Unocic, and M.J. Mills are with The Ohio State University, 2041 College Road, Columbus, OH 43210, and J. Li is with the University of Pennsylvania, 3231 Walnut Street, Philadelphia, PA 19104. Prof. Mills can be reached at mills.108@osu.edu.